24

Magnetic Properties and Size Effects of Spin-1/2 and Spin-1 Models of Core-Surface Nanoparticles in Different Type Lattices

Orhan Yalçın[1], Rıza Erdem[2] and Zafer Demir[3]
[1]Department of Physics, Niğde University, Niğde
[2]Department of Physics, Akdeniz University, Antalya
[3]Institute of Graduate School of Natural and Applied Sciences, Niğde University, Niğde
Turkey

1. Introduction

Dimension in the range of 1 to 100 nm, is called the nano regime. In recent years, nanoparticles/quantum dots are in a class of magnetic nanostructures (Aktaş et al., 2003, 2006; Kartopu & Yalçın, 2010). Nanoparticles (NPs) have been steadily interesting in Physics, Chemistry, Biology, Biomedicine, Spintronics, etc. As the dimensions of magnetic NPs decrease down to the nanometer scale, these core-surface NPs start to exhibit new and interesting physical properties mainly due to quantum size effects. Even the intrinsic physical characteristics of NPs are observed to change drastically compared to their macroscopic counterparts. The potential applications of NPs are very attractive for magneto-sensor, bio-sensor, magneto-electronics, data storage media, computer hard disks, microwave electronic devices, nano-transistors, etc. Especially, the studies of core-surface NPs are extremely important for technology because of transmission of data at high density to optical computer, nanorobot to assemble, compose rigid disk. The nanoparticles have relevance to thin film devices in the new breed of magnetoelectronics, spin-valve, spin-transistors, spin-dependence tunneling devices and etc. (Babin, et al., 2003). The hysteresis in fine magnetic particles applied to new technologies such as Magnetic Random Access Memory (MRAM).

In generally, a nanoparticle is divided into the inner, outer and intermediate regions. These zones are called core (C), surface (S) and core-surface (CS), respectively. The size effects of core-surface NPs are very important for technological and biomedicine applications (Fraerman et al., 2001; Pankhurst et al., 2003). Especially, superparamagnetic (single-domain) NPs are important for non surgecial interfere of human body. The ferromagnetic (FM) orders in magnetic systems were dominated as mono-domain (or single-domain) nanoparticles consisting of FM surface and antiferromagnetic (AFM) core regions which couple with each other (Rego & Figueiredo, 2001; Leite & Figueiredo, 2004). At the lower temperatures, the FM surface and AFM core are only ordered in the noninteracting (monodomain) NPs. Stoner-Wohlfarth (Stoner & Wohlfarth, 1948) and Heisenberg model (Heisenberg, 1928) to describe the fine structure were fistly used in detail. Magnetic evolutions with temperatures (Babin, et al., 2003; Szlaferek, 2004; Usov & Gudoshnikov, 2005), thermodynamic properties (Vargas et al., 2002) and experimental techniques (Wernsdorfer et al., 1995; Wernsdorfer et al., 2000) were performed by different type works for the core-surface NPs. A simple (Bakuzis & Morais, 2004) and the first atomic-scale models of the ferrimagnetic and heterogeneous systems in which the exchange energy plays a central role in determining the magnetization of the NPs, were studied (Kodama et al., 1996, 1999; Kodama & Berkowitz, 1999).

Ising models and real magnets have provided a rich and productive field for the interaction between theory and experiment over the past 86 years (Ising, 1925; Peierls, 1936). Ising models (Erdem, 1995; Keskin, & Erdem 1997; Erdem & Keskin, 2001; Erdem, 2009; Erdem, 2008; Chen & Levy, 1973) and thier variants such as Blume-Capel (Blume, 1966; Capel, 1966; Bakchich, et al., 1994), Blume-Emery-Griffiths (Blume, et al., 1971; Achiam, 1985; Hoston, & Berker, 1991; Bakkali, 1996; Goveas & Mukhopadhyay, 1997; Keskin, et al., 1999; Temizer, 2008) and mixed spin (Benayad & Dakhama 1997; Kaneyoshi, 1998; Albayrak, & Yigit, 2005; Albayrak, & Yigit, 2006; Albayrak, 2007; Albayrak, 2007; Deviren, et al., 2009) models were regarded as theoretical simplifications, designed to model the essential aspects of cooperative system (Kikuchi,1951) without detailed correspondence to specific materials.

In the scope of this chapter, we give a detailed analysis for both spin $S=1/2$ and $S=1$ Ising models of homegeneous and core-surface composite NPs to describe the magnetic properties of these particles. These models are based on the pair approximation in the Kikuchi version (Kikuchi, 1974; Keskin, 1986; Erdinç & Keskin, 2002; Yalçın, et al. 2008, Özüm, 2010; Çiftçi, 2011). Incorporating the pair correlations between the spins inside the NPs, we calculated the free energy and minimized with respect to pair variables to obtain the field-cooled magnetization. The field cooling magnetization (*M*) curves of homogeneous and composite NPs are given as a function of the reduced temperature with different radius and different type lattices. Hysteresis loops and coercive fields with their linear fit to the data were plotted as a function of radius and temperature of different NPs. We compared our result with other works (Kaneyoshi, 2005; Kodama, 1999; Usov & Gudoshnikov, 2005).

2. Theoretical model

2.1 Ising model

Ising model, which was introduced in the field of magnetism, is one of the most studied models in modern statistical physics. Although its greatest success during the last century has been in the theory of phase transitions, the model today is viewed as a mathematical structure which can represent a variaty of different physical phenomena. In this section, we give a brief summary for the basics of the model before its application to the nanoparticle (NP) magnetism.

Ising model is considered on a regular lattice where each interior site has the same number of nearest-neighbour sites. This is called the coordination number of the lattice and will be denoted by γ. The system under consideration is composed of the magnetic atoms (also called the spins) located at the lattice sites. It is assumed that, in the thermodynamic limit, boundary sites can be disregarded and that, with N sites, the number of nearest-neighbour site pairs is $N\gamma/2$. The standard Hamiltonian for the the simplest Ising model is given by

$$\mathrm{H}\{S_i\} = -J\sum_{\langle ij\rangle} S_i S_j - h\sum_{\langle ij\rangle}(S_i + S_j)\text{, with } S_i = \pm 1\text{,} \tag{1}$$

where h is the external magnetic field at the site i and the summation is performed for nearest-neighbour sites. J is the exchange interaction between neighbouring sites $\langle ij\rangle$. Two distinctive cases corresponding to different signs of intersite interaction is considered, i.e., $J < 0$ (ferromagnetic (FM) coupling) and $J > 0$ (antiferromagnetic (AFM) coupling). The fractions of $S_i = \pm 1$ spins given by X_i are called the point (or state) variables. The X_i are normalized by $\sum_{i=1}^{2} X_i = 1$. The long-range order parameter in the model is called the magnetization (M) and it is defined by $M = X_1 - X_2$. From this definition and the normalization condition the point variables can be written as

$$X_1 = \frac{1}{2}(1+M)\text{, } X_2 = \frac{1}{2}(1-M)\text{.} \tag{2}$$

On the other hand, Eq. (1) may be extended by allowing values $s = 0, \pm 1, \pm 2, \ldots, \pm S$ for the variables. It is then possible to consider higher order interactions such as $K\sum_{\langle ij\rangle} S_i^2 S_j^2$ or a chemical potential such as $\Delta\sum_i S_i^2$. These generalizations are regarded as extensions of the Blume-Emery-Griffiths (BEG) model (Blume et al., 1971). Recently, there have been many theoretical studies of mixed spin Ising systems. These are of interest because they have less translational symmetry than their single-spin counterparts since they consist of two interpenetrating inequivalent sublattices. The latter property is very important to study a certain type of ferrimagnetism, namely molecular-based magnetic materials which are of current interest (Kaneyoshi et al., 1998).

2.2 Pair approximation

In the pair approximation, we consider the pair correlations between the spins. Besides the point variables (X_i), we introduce new variables (Y_{ij}), indicating the average number of the states in which the first member of the nearest-neighbour pair is in state i and the second member in state j. These will be called the pair or bond variables. The bond variables are normalized by $\sum_{i,j=1}^{n} Y_{ij} = 1$ and related to the state varibales by the relations $X_i = \sum_{j=1}^{n} Y_{ij}$. Here n is the number of spin states in the given spin S model. The interaction energy E and entropy S_E can be written in terms of Y_{ij} as

$$\beta E = N\frac{\gamma}{2}\sum_{i,j}^{n} \eta_{ij} Y_{ij}\text{ ,} \tag{3}$$

$$S_E = Nk\left((\gamma - 1)\sum_{i,j=1}^{n} X_i \ln(X_i) - \frac{\gamma}{2}\sum_{i,j=1}^{n} Y_{ij}\ln(Y_{ji})\right)\text{,} \tag{4}$$

where $\beta = 1/kT$ (k Boltzmann's constant and T temperature). In Eq. (3), the parameters η_{ij} are called the bond energies for the spin pairs (i, j) and determined from Eq. (1). The free energy per site Φ can be found from

$$\Phi = \frac{\beta F}{N} = \frac{\beta}{N}(E - TS_E)\,. \tag{5}$$

For the system at equilibrium, the minimization of Eq. (5) with respect to Y_{ij} ($\partial\Phi / \partial Y_{ij} = 0$) leads to the following set of self-consistent equations:

$$Y_{ij} = \frac{1}{Z}(X_i X_j)^{\bar{\gamma}}\, e^{-\beta \eta_{ij}} \equiv \frac{e_{ij}}{Z}\,, \tag{6}$$

where $\bar{\gamma} = (\gamma - 1)/\gamma$ and Z is the partition function:

$$Z = \exp(2\beta\lambda / \gamma) = \sum_{i,j=1}^{n} e_{ij}\,. \tag{7}$$

In Eq. (7), λ is introduced to maintain the normalization condition. Applications of the above formulation to $S = 1/2$ and $S = 1$ Ising systems can be found in many works in the literature (Meijer et al., 1986; Keskin & Meijer, 1986; Keskin & Erdinç, 1995; Erdinç & Keskin, 2002). These applications are summerized for comparison in Table 1.

	$S = 1/2$	$S = 1$
Spin state variables (X_i)	X_1, X_2	X_1, X_2, X_3
Spin values (S_i)	$+1$, -1	$+1$, 0, -1
Bond variables $Y_{ij}(S_i, S_j)$	$Y_{11}(+1,+1), Y_{12}(+1,-1)$ $Y_{21}(-1,+1), Y_{22}(-1,-1)$	$Y_{11}(+1,+1), Y_{12}(+1,0), Y_{13}(+1,-1)$ $Y_{21}(0,+1), Y_{22}(0,0), Y_{23}(0,-1)$ $Y_{31}(-1,+1), Y_{32}(-1,0), Y_{33}(-1,-1)$
Normalization	$\sum_{i=1}^{2} X_i = 1,\ \sum_{i,j=1}^{2} Y_{ij} = 1$	$\sum_{i=1}^{3} X_i = 1,\ \sum_{i,j=1}^{3} Y_{ij} = 1$
Relations between point variables and pair variables	$X_i = \sum_{j=1}^{2} Y_{ij}$	$X_i = \sum_{j=1}^{3} Y_{ij}$
	$X_1 = Y_{11} + Y_{12}$ $X_2 = Y_{21} + Y_{22}$	$X_1 = Y_{11} + Y_{12} + Y_{13}$ $X_2 = Y_{21} + Y_{22} + Y_{23}$ $X_3 = Y_{31} + Y_{32} + Y_{33}$
Avarage magnetization ($M \equiv \langle S_i \rangle$)	$M = X_1 - X_2$	$M = X_1 - X_3$
	$M = Y_{11} + Y_{12} - (Y_{21} + Y_{22})$	$M = Y_{11} + Y_{12} + Y_{13}$ $-(Y_{31} + Y_{32} + Y_{33})$
Quadrupole moment $Q \equiv \langle Q \rangle \equiv \langle S_i^2 \rangle$	-----	$Q \equiv X_1 + X_3$
		$Q = Y_{11} + Y_{12} + Y_{13} + Y_{31} + Y_{32} + Y_{33}$

Table 1. Comparison of the $S = 1/2$ and $S = 1$ Ising models under the pair approximation.

3. Magnetic properties of $S = 1/2$ and $S = 1$ Ising nanoparticles

The magnetic particles become single domain below a critical size in contrast with the usual multidomain structure of the bulk materials. Therefore, in the scope of this section, we study size effects and magnetic properties of monodomain NPs manifestations. We consider a noninteracting monodomain NP with Ising spins on both hexagonal and square lattices for any two-dimensional (2D) regular arrays which can also be extended to hexagonal closed packed (hcp) and simple cubic (sc) lattices for the three-dimensional (3D) case as in Fig.1. The shells and their numbers originate from the nearest-neighbor pair interactions for the hexagonal and square lattices in 2D. In this structure, number of shells for hexagonal and square lattices can be associated with radius (R) of the NPs. This behaviour can be seen explicitly in Fig. 2 for hexagonal lattice and in Fig. 3 for square lattice. The value of R includes number of shells and the size of a NP increases as the number of shells increses. Therefore, we have considered Ising spins in three parts that are core (C), core-surface (CS) and surface (S) within the NP. Each of these parts contain core spin number (N_C), core-surface spin number (N_{CS}) and surface spin number (N_S), respectively. The total number of spins (N) in a single NP involves core and surface spin numbers, i.e. $N = N_C + N_S$. The C and S spins interact ferromagnetically $(J < 0)$ or antiferromagnetically $(J > 0)$. The $S = 1/2$ and $S = 1$ Ising model Hamiltonians with dipol-dipol interaction (J) for a NP is given by

$$\mathrm{H} = \mathrm{H_C} + \mathrm{H_{CS}} + \mathrm{H_S} \, , \tag{8}$$

with

$$\mathrm{H}_C = -J_C \sum_{\langle i,j \rangle} S_i S_j - h \sum_{\langle i,j \rangle} (S_i + S_j) \, ,$$

$$\mathrm{H}_{CS} = -J_{CS} \sum_{\langle i,j \rangle} S_i \sigma_j \, , \tag{9}$$

$$\mathrm{H}_S = -J_S \sum_{\langle i,j \rangle} \sigma_i \sigma_j - h \sum_{\langle i,j \rangle} (\sigma_i + \sigma_j) \, ,$$

where J_C, J_{CS} and J_S represent exchange interactions for C, CS and S atoms, respectively. If $J_C = J_{CS} = J_S$, the NP is known as a homegeneous NP. It is called a composite NP when $J_C \neq J_{CS} \neq J_S$, $J_C = J_{CS} \neq J_S$, $J_C \neq J_{CS} = J_S$ or $J_{CS} \neq J_C = J_S$. In Eqs. (9), S_i is called the core spin values and σ_i is the surface spin values. These variables take on the values ± 1 for $S = 1/2$ and $0, \pm 1$ for $S = 1$ Ising systems.

The interaction energies for $S = 1/2$ and $S = 1$ models of an Ising NP in 2D can be written shortly in term of Y_{ij} as

$$\beta E = \sum_{\langle i,j \rangle} (N_P^C \eta_{ij}^C + N_P^{CS} \eta_{ij}^{CS} + N_P^S \eta_{ij}^S) Y_{ij} \, , \tag{10}$$

where the numbers of spin pairs for C, CS and S regions are defined by $N_P^C = (N_C\gamma_C/2) - N_{CS}$, $N_P^{CS} = 2N_{CS}\gamma_{CS}/2$ and $N_P^S = N_S\gamma_S/2$, respectively. Similarly γ_C, γ_{CS}, γ_S denote the coordination numbers for these regions. Since we consider the arrays of Ising spins for a structure made up of bigger particles in 2D, we choose $\gamma_C = 6$, $\gamma_{CS} = \gamma_S = 2$ for hexagonal lattice and $\gamma_C = 4$, $\gamma_S = 0$, $\gamma_{CS} = 2$ for square lattice, as depicted in Figs. 2 and 3, respectively. The values of these numbers for both suructures in 2D are given in Table 2. The expressions for the bond energies η_{ij}^C, η_{ij}^{CS} and η_{ij}^S of three regions are found using Eq. (9) for both models, as listed in Table 3.

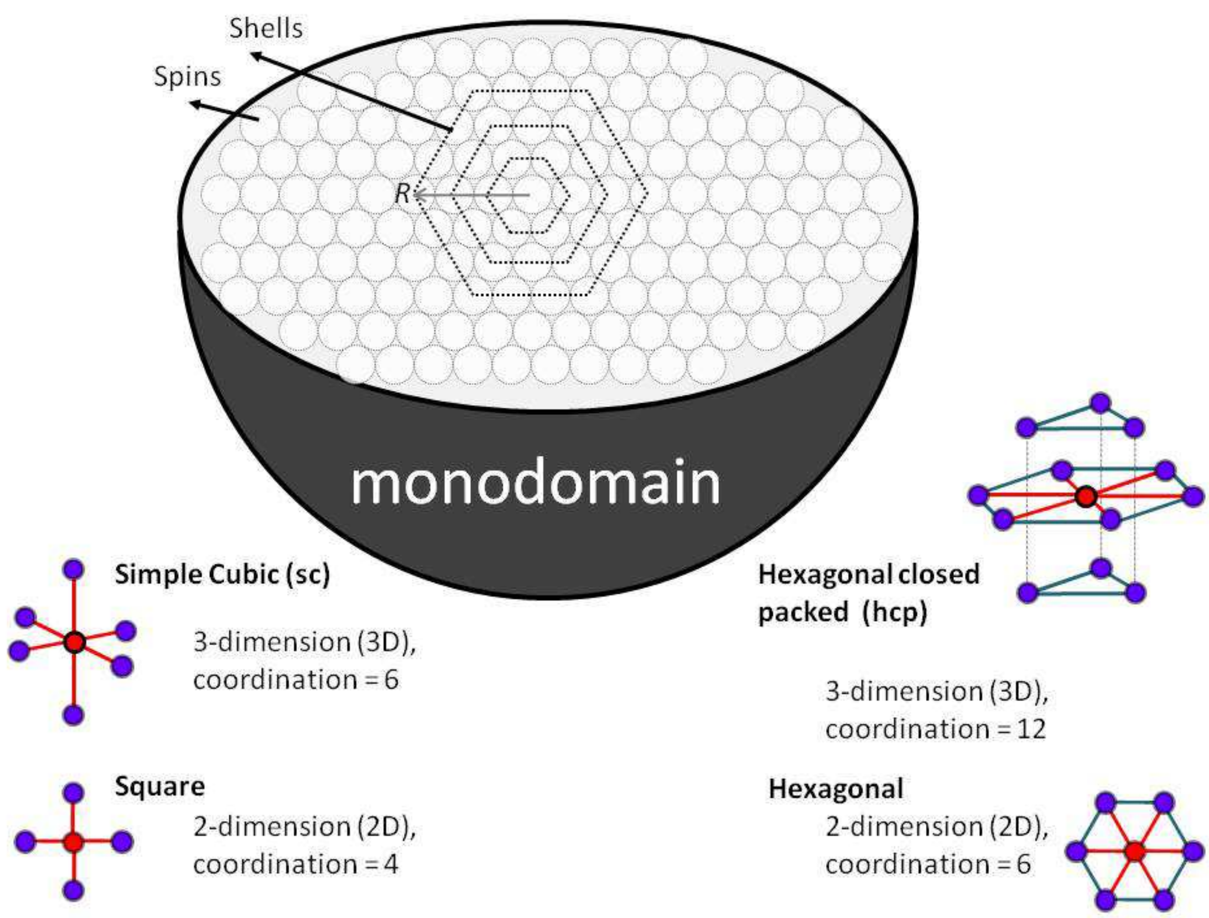

Fig. 1. A spherical monodomain magnetic NP spaced coherently in a form of 3D arrays. The shape of a single NP consists of the hexagonal lattice. The dashed lines displayed shells of spins in a 2D finite arrays. The radius of NP (R) includes shell numbers. The insets exhibit coordination numbers (γ) of hexagonal closed packed (hcp) and simple cubic (sc) lattices in 3D as well as hexagonal and square lattices in 2D structure.

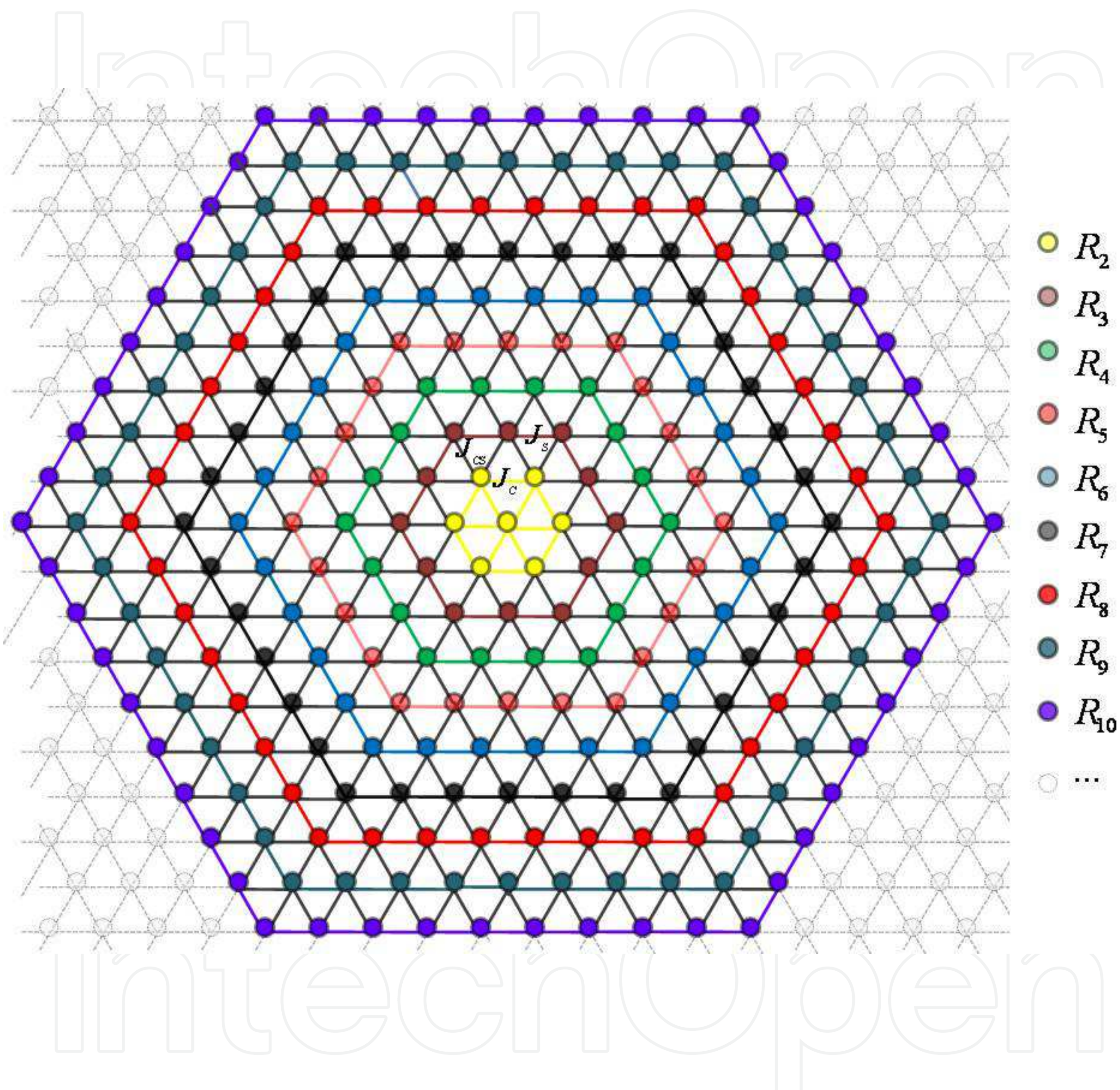

Fig. 2. Schematic representation of a NP on a hexagonal lattice in 2D exhibiting nine shells of spins. Small full coloured circles correspond to ten radius of the NP. Solid grey lines are number of the core-shell pairs. Solid coloured lines are number of shell pair (this line corresponds to core and shell number for $R = 2$).

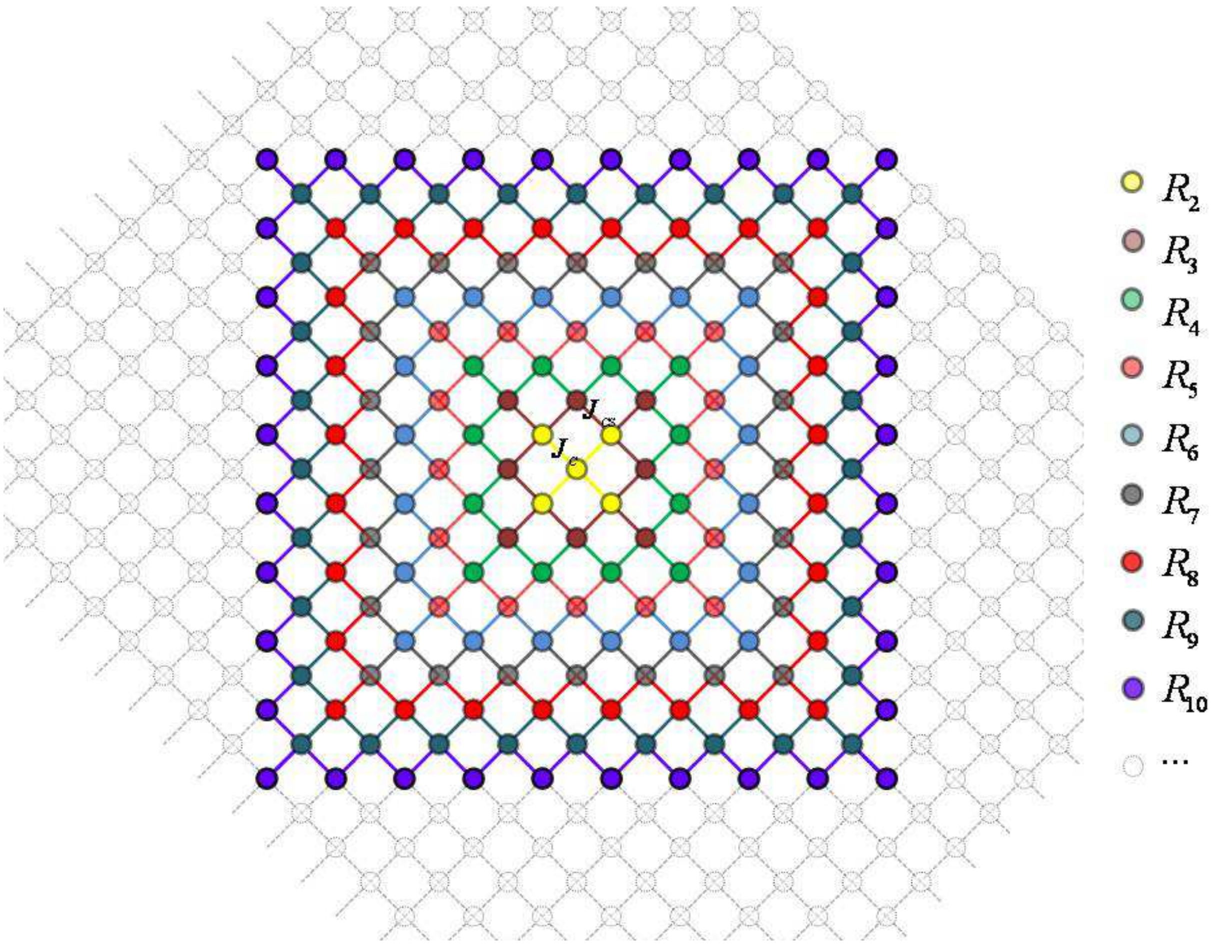

Fig. 3. Same as Fig. 2 but for the NP on square lattice in 2D.

Lattice Type	R	2	3	4	5	6	7	8	9	10
Hexagonal Lattice in 2D	N_C	7	19	37	61	91	127	169	217	271
	N_S	12	18	24	30	36	42	48	54	60
	N_{CS}	9	15	21	27	33	39	45	51	57
	N_P^C	12	42	90	156	240	342	462	600	756
	N_P^S	12	18	24	30	36	42	48	54	60
	N_P^{CS}	18	30	42	54	66	78	90	102	114
Square Lattice in 2D	N_C	5	13	25	41	61	85	113	145	181
	N_S	8	12	16	20	24	28	32	36	40
	N_{CS}	6	10	14	18	22	26	30	34	38
	N_P^C	4	16	36	64	100	144	196	256	324
	N_P^{CS}	12	20	28	36	44	52	60	68	76

Table 2. Numbers of the spins and spin pairs within the C, CS and S regions (Yalçın, et al., 2008).

Spin Model	Pair	Bond energy for Core (η_{ij}^{C})	Bond energy for Core –Surface (η_{ij}^{CS})	Bond energy for Surface (η_{ij}^{S})
$S=1/2$ ($n=2$)	η_{11}	$-J_C-2h$	$-J_{CS}$	$-J_S-2h$
	η_{12}	$+J_C$	$+J_{CS}$	$+J_S$
	η_{21}	$+J_C$	$+J_{CS}$	$+J_S$
	η_{22}	$-J_C+2h$	$-J_{CS}$	$-J_S+2h$
$S=1$ ($n=3$)	η_{11}	$-J_C-2h$	$-J_{CS}$	$-J_S-2h$
	η_{12}	$-h$	0	$-h$
	η_{13}	$+J_C$	$+J_{CS}$	$+J_S$
	η_{21}	$-h$	0	$-h$
	η_{22}	0	0	0
	η_{23}	$+h$	0	$+h$
	η_{31}	$+J_C$	$+J_{CS}$	$+J_S$
	η_{32}	$+h$	0	$+h$
	η_{33}	$-J_C+2h$	$-J_{CS}$	$-J_S+2h$

Table 3. Bond energies for $S=1/2$ and $S=1$ models.

Using Eq. (6) we obtain four self-consistent equations of Y_{ij} for $S=1/2$ model of core-surface NPs:

$$\begin{aligned}
Y_{11} &= \frac{1}{Z}\left(X_1X_1\right)^{\bar{\gamma}} \exp\left[-\beta\left(N_P^C\eta_{11}^C + N_P^{CS}\eta_{11}^{CS} + N_P^S\eta_{11}^S\right)\right] \equiv \frac{e_{11}}{Z},\\
Y_{12} &= \frac{1}{Z}\left(X_1X_2\right)^{\bar{\gamma}} \exp\left[-\beta\left(N_P^C\eta_{12}^C + N_P^{CS}\eta_{12}^{CS} + N_P^S\eta_{12}^S\right)\right] \equiv \frac{e_{12}}{Z},\\
Y_{21} &= \frac{1}{Z}\left(X_2X_1\right)^{\bar{\gamma}} \exp\left[-\beta\left(N_P^C\eta_{21}^C + N_P^{CS}\eta_{21}^{CS} + N_P^S\eta_{21}^S\right)\right] \equiv \frac{e_{21}}{Z},\\
Y_{22} &= \frac{1}{Z}\left(X_2X_2\right)^{\bar{\gamma}} \exp\left[-\beta\left(N_P^C\eta_{22}^C + N_P^{CS}\eta_{22}^{CS} + N_P^S\eta_{22}^S\right)\right] \equiv \frac{e_{22}}{Z}.
\end{aligned} \tag{11}$$

Similarly, nine self-consistent equations of Y_{ij} for $S=1$ model of these particles are

$$
\begin{aligned}
Y_{11} &= \frac{1}{Z}(X_1X_1)^{\bar{\gamma}} \exp\left[-\beta\left(N_P^C\eta_{11}^C + N_P^{CS}\eta_{11}^{CS} + N_P^S\eta_{11}^S\right)\right] \equiv \frac{e_{11}}{Z}, \\
Y_{12} &= \frac{1}{Z}(X_1X_2)^{\bar{\gamma}} \exp\left[-\beta\left(N_P^C\eta_{12}^C + N_P^{CS}\eta_{12}^{CS} + N_P^S\eta_{12}^S\right)\right] \equiv \frac{e_{12}}{Z}, \\
Y_{13} &= \frac{1}{Z}(X_1X_3)^{\bar{\gamma}} \exp\left[-\beta\left(N_P^C\eta_{13}^C + N_P^{CS}\eta_{13}^{CS} + N_P^S\eta_{13}^S\right)\right] \equiv \frac{e_{13}}{Z}, \\
Y_{21} &= \frac{1}{Z}(X_2X_1)^{\bar{\gamma}} \exp\left[-\beta\left(N_P^C\eta_{21}^C + N_P^{CS}\eta_{21}^{CS} + N_P^S\eta_{21}^S\right)\right] \equiv \frac{e_{21}}{Z}, \\
Y_{22} &= \frac{1}{Z}(X_2X_2)^{\bar{\gamma}} \exp\left[-\beta\left(N_P^C\eta_{22}^C + N_P^{CS}\eta_{22}^{CS} + N_P^S\eta_{22}^S\right)\right] \equiv \frac{e_{22}}{Z}, \\
Y_{23} &= \frac{1}{Z}(X_2X_3)^{\bar{\gamma}} \exp\left[-\beta\left(N_P^C\eta_{23}^C + N_P^{CS}\eta_{23}^{CS} + N_P^S\eta_{23}^S\right)\right] \equiv \frac{e_{23}}{Z}, \\
Y_{31} &= \frac{1}{Z}(X_3X_1)^{\bar{\gamma}} \exp\left[-\beta\left(N_P^C\eta_{31}^C + N_P^{CS}\eta_{31}^{CS} + N_P^S\eta_{31}^S\right)\right] \equiv \frac{e_{31}}{Z}, \\
Y_{32} &= \frac{1}{Z}(X_3X_2)^{\bar{\gamma}} \exp\left[-\beta\left(N_P^C\eta_{32}^C + N_P^{CS}\eta_{32}^{CS} + N_P^S\eta_{32}^S\right)\right] \equiv \frac{e_{32}}{Z}, \\
Y_{33} &= \frac{1}{Z}(X_3X_3.)^{\bar{\gamma}} \exp\left[-\beta\left(N_P^C\eta_{33}^C + N_P^{CS}\eta_{33}^{CS} + N_P^S\eta_{33}^S\right)\right] \equiv \frac{e_{33}}{Z}.
\end{aligned} \tag{12}
$$

Eqs. (11) and (12) are solved numerically using Newton-Raphson method and normalized magnetization (M) is easily calculated for both $S=1/2$ and $S=1$ models of homegeneous and core-surface composite NPs. Results are shown as the magnetization curves and hysteresis loops in Figs. 4–9.

4. Result and discussions

4.1 Magnetization

The evolution of normalized magnetization (M) as a function of the reduced temperature ($k_B T / J_0$) and particle size dependence of the transition temperature T_C from FM to paramagnetic (PM) phases for homogeneous and composite Ising NPs are shown in Figs. 4 and 5, respectively. The magnetization curves in Fig. 4 are plotted for $S=1/2$ and $S=1$ models of homogeneous NPs using the FM core ($J_0=1$, $J_C=1$), FM surface ($J_S=J_0$) and FM core-surface ($J_{CS}=J_0$) interactions and the curves in Fig. 5 are obtained for both models of the composite NPs based on FM core ($J_C=J_0$), FM surface ($J_S=J_0$) and AFM core-surface ($J_{CS}=-J_0$) interactions. In the plots, different values for the applied magnetic field are considered ($h=0.0\text{-}0.1$). The solid curves in the figures correspond to hexagonal lattice while dotted ones denote the square lattice. As seen from the figures, the changes in the magnetization with the reduced temperature point out an interesting aspect for NPs on the hexagonal and square lattices in 2D. The magnetization curves are decreasing from one (1) to zero (0) value while the reduced temperature is increasing (Figs. 4(a), 4(b), 5(a), 5(b)). These decreases terminate at the phase transition temperature (or Curie temperature, T_C) from FM phase to PM phase for $h=0.0$, seen in Figs. 4(c) and 5(c). To show the size dependence of the critical temperature we plot $\sqrt{T_C}$ vs R in Figs. 4(d) and 5(d). All critical temperature values follow a linear increase with the particle radius. With increase in the particle radius it approaches to the Crue temperatures of the bulk materials. This is consistent with the mean-field approximation for the magnetic structure of Heisenberg NP (Usov & Gudoshnikov, 2005). On the other hand, it is interesting that composite $S = 1/2$ and $S = 1$ Ising NPs show smaller transition temperatures than their corresponding homegeneous NPs. This can easily be seen by comparing the same coloured fits in Figs. 4(d) and 5(d).

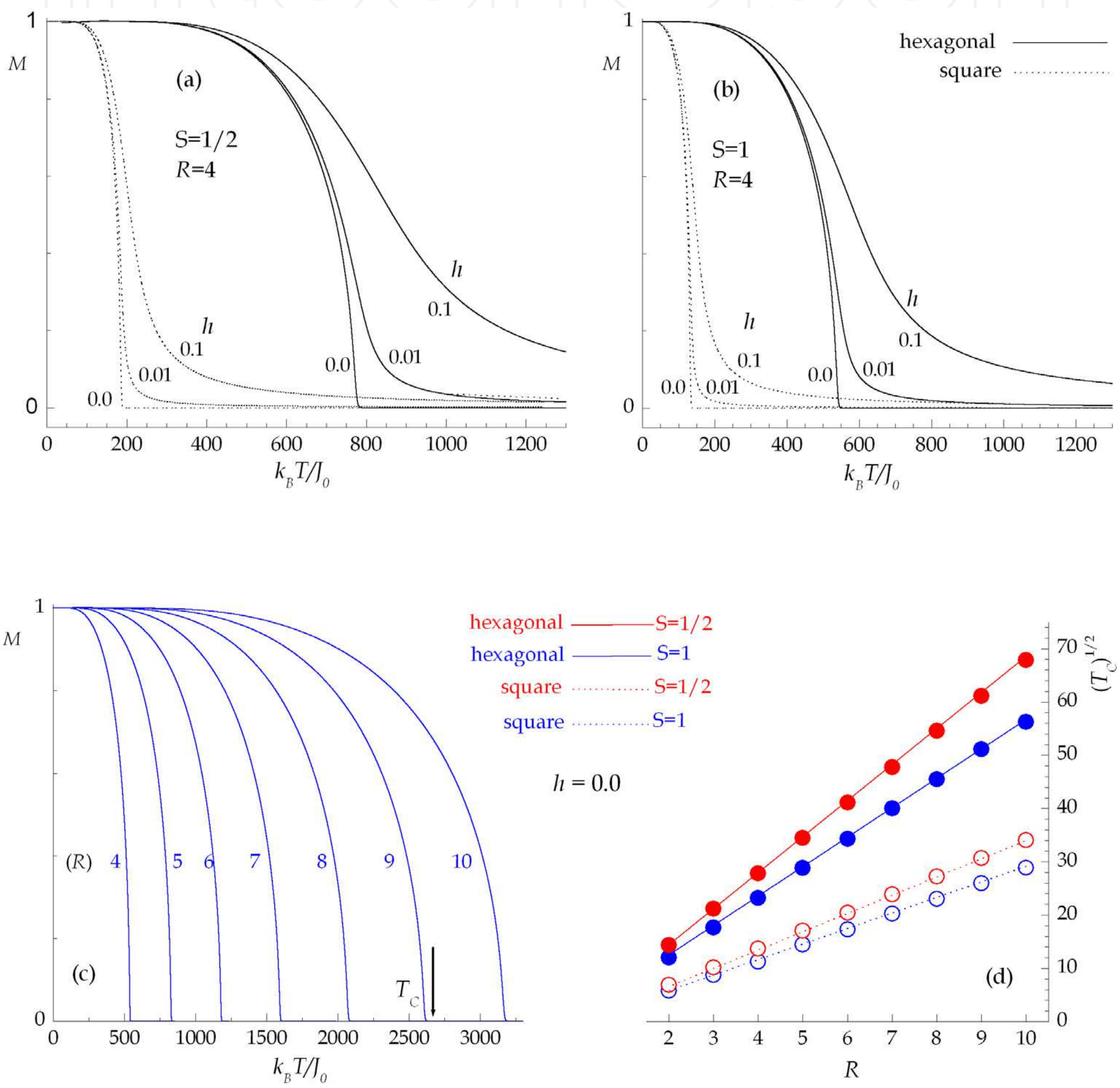

Fig. 4. Normalized magnetization (M) vs. reduced temperature (k_BT / J_0) and particle size dependence of the transition temperature T_C from FM to PM phases for homogeneous $S = 1/2$ and $S = 1$ Ising NPs on the hexagonal and square lattices. $J_0 = J_C = J_{CS} = J_S = 1$ and $h = 0.0$-0.1.

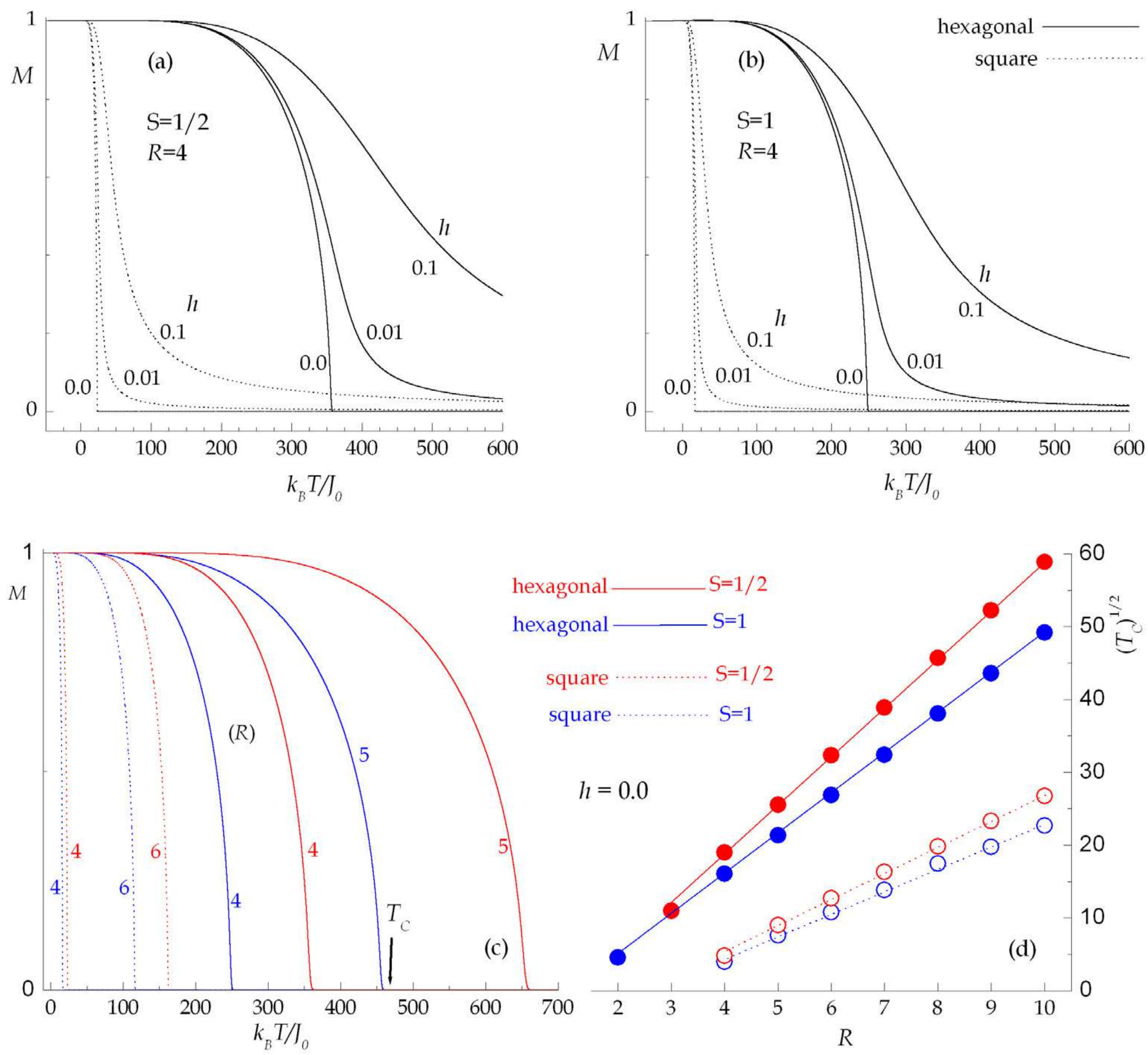

Fig. 5. Same as Fig. 4 but for the core-surface composite NPs with $J_0 = J_C = J_S = 1,\ J_{CS} = -J_0 = -1.$

4.2 Hysteresis loops

The magnetic field evolution of normalized magnetization (or hysteresis loops) for the homegeneous $S = 1/2$ and $S = 1$ Ising NPs which has different particle sizes and their corresponding coercive field vs. R^{-2} variation are given Figs. 6 and 7, respectively. We consider a FM coupling in core $(J_C = J_0)$, surface $(J_S = J_0)$ and core-surface $(J_{CS} = J_0)$ regions with $J_0 = 1$ on the hexagonal and square lattice structures. The hysteresis curves of small diameters, namely with radius $R = 2,4,5$ in Figs. 6(a)-6(d), are approximately the same. These behaviours are called superparamegnetic (SP) regime. However, the loops strongly depend on the size of NP. The hysteresis curves of high diamater values change sharply, as also shown in Figs. 6(a)-6(d). Moreover, the hysteresis curves for this type of NPs are broadening while the diamater of NPs is increasing so that it approaches to bulk materials. The size dependence of the coercive fields h_C is determined from the hysteresis loops in Fig. 7. In Fig. 7, the full red and blue circles correspond to the curves obtained for $R = 2-9$ in the Figs. 6(a) and 6(c), respectively. Similarly, the open red and blue circles correspond to the curves obtained for $R = 3-11$ and $R = 4-10$ in Figs. 6(b) and 6(d), respectively. The straight solid and dotted lines are the results from a linear fit to the calculated data. From this fit, it is obvious that the coercive field (h_C) depends linearly on $1/R^2$.

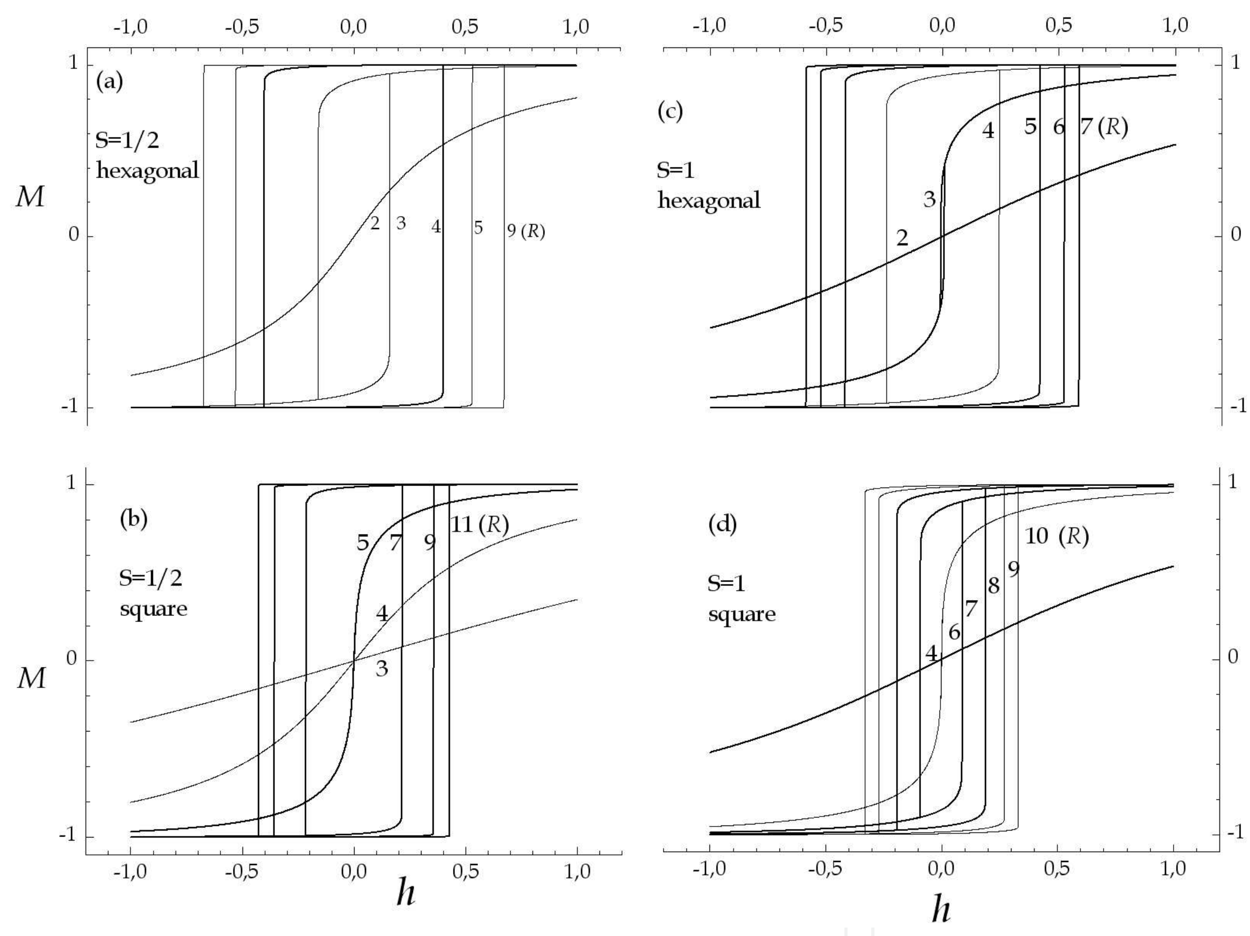

Fig. 6. (a) Hysteresis loops of a homegeneous $S = 1/2$ Ising NP on the hexagonal lattice for various sizes. (b) Same as Fig. 6(a) but for NP on the square lattice. (c) Hysteresis loops of a homegeneous $S = 1$ Ising NP on the hexagonal lattice for different sizes. (d) Same as Fig. 6(c) but for NP on the square lattice. $J_0 = J_C = J_{CS} = J_S = 1$ and $T = 300 J_0/k_B$.

Magnetic hysteresis loops of composite $S = 1/2$ and $S = 1$ Ising NPs on the hexagonal and square lattice (in 2D) structures for various values of particle sizes are shown in Fig. 8. The exchange interactions in the C and S regions are FM, i.e. $J_0 = J_C = J_S$, while the coupling between C and S is an AFM exchange constant $J_{CS} = -J_0$ for each type of NP. From the figure, it is clear that the hysteresis loops strongly depend on the particle size. The loops for the $S = 1/2$ and $S = 1$ Ising NPs on the hexagonal lattice change suddenly in low radius values while those for the $S = 1/2$ and $S = 1$ Ising NPs on the square lattice in high radius values.

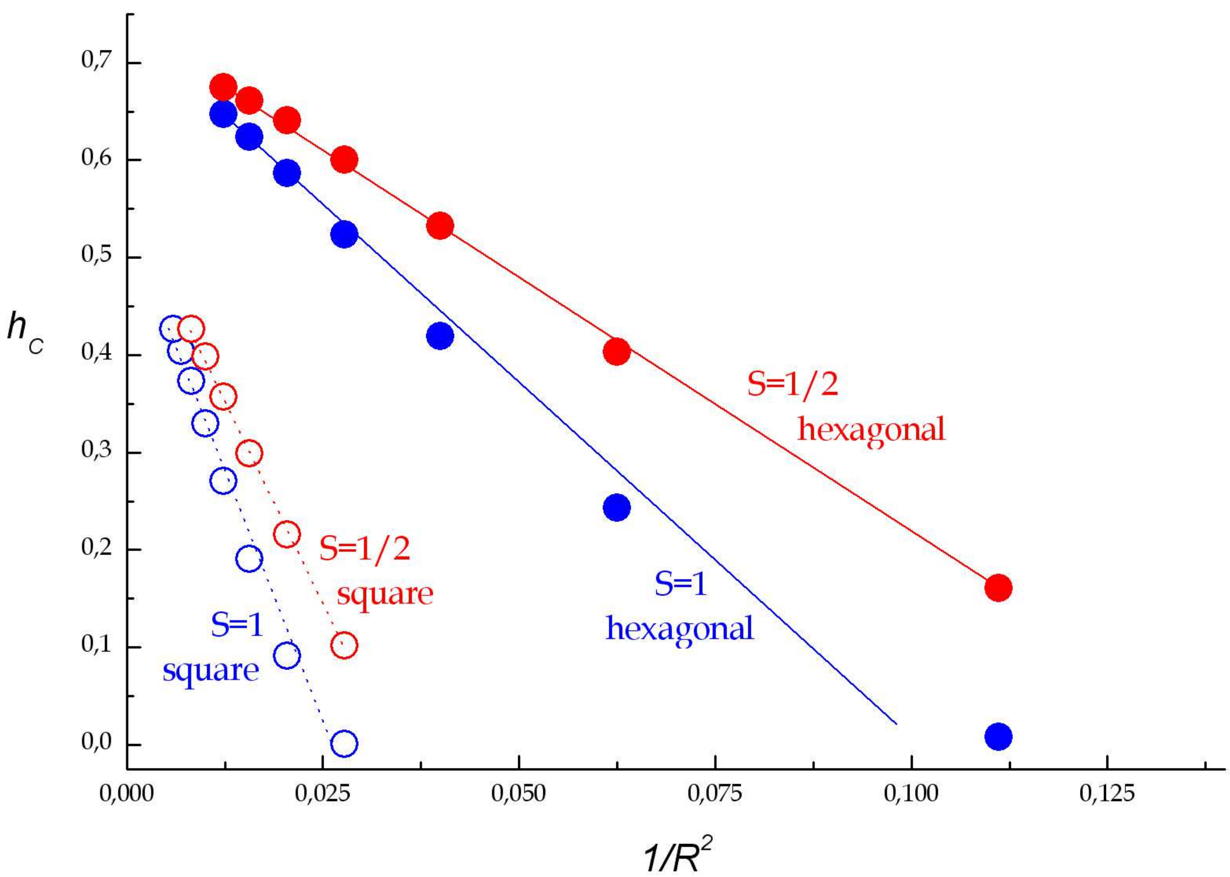

Fig. 7. The coercive field (h_C) plotted as a function of R^{-2} for the hysteresis loops of the homegeneous NP in Fig. 6.

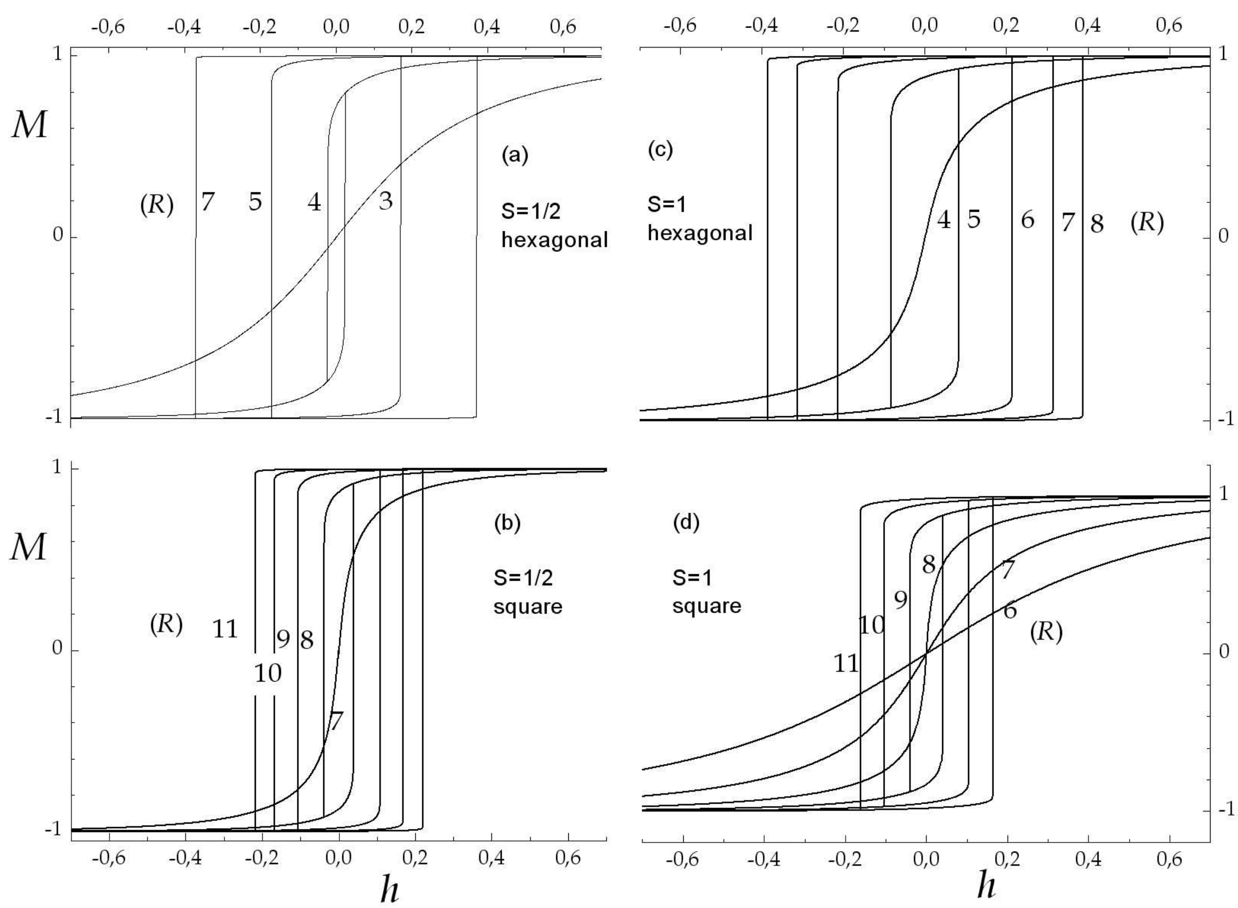

Fig. 8. Same as Fig. 6 but for the composite NP. $J_0 = J_C = J_S = 1$, $J_{CS} = -J_0$.

Finally, the evolutions of hysteresis loops and their coercive field according to the temperature of composite Ising NPs are seen to change monotically as the temperature increases, illustrated in Fig. 9(a) and 9(b), respectively. Since the loops for both models of NPs on the hexagonal and square lattices display the same behaviour we have drawn only the loops of $S = 1/2$ Ising NP on the hexagonal lattice. In this case, hysteresis for the NP is in superparamagnetic (SP) regime at $700 J_0 / k_B$. But, the loops for the temperature regime between $150 J_0/k_B$ - $600 J_0 / k_B$ belong to the FM phase (Fig. 9(a)). The tempereture dependence of the coercivity (h_C) are determined from the hysteresis loops of Fig. 9(a), as given in Fig. 9(b).

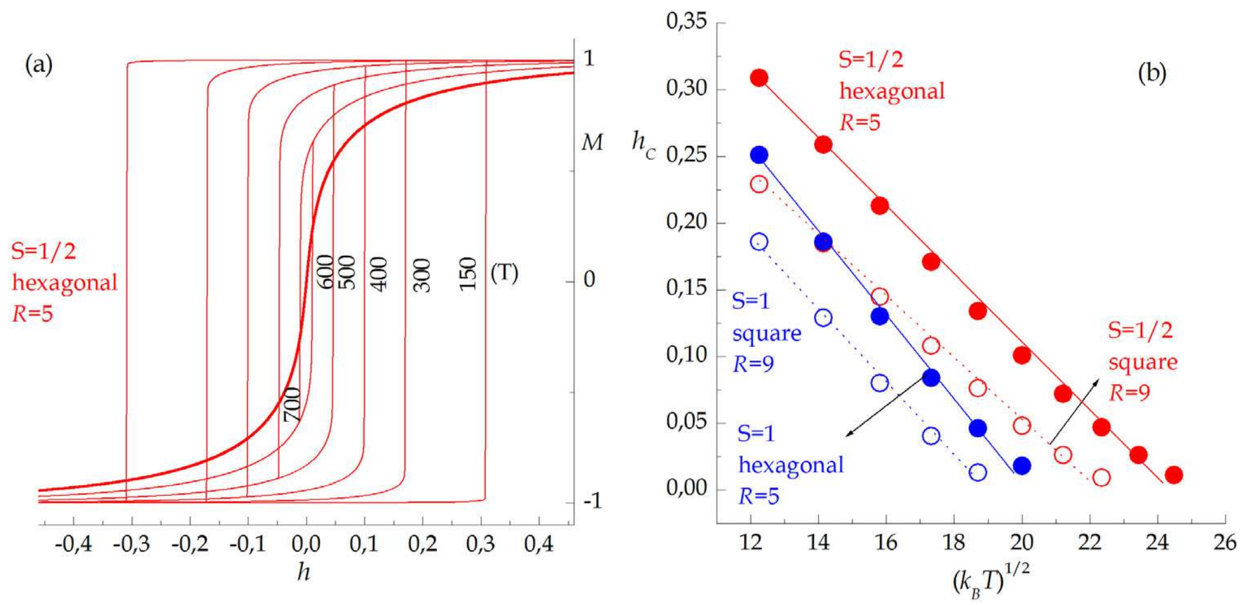

Fig. 9. (a) Temperature dependence of the hysteresis loops for the $S = 1/2$ Ising NP on the hexagonal lattice exhibiting five shells of spins ($R = 5$). (b) The coercive field (h_C) plotted as function of $(k_B T)^{1/2}$ for two models of NP on both structures studied above. $J_0 = J_C = J_S = 1,\ J_{CS} = -J_0$.

5. Conclusion

In the scope of this chapter, we have focused on the magnetic properties with size effects for homogeneous and core-surface composite NPs which have Ising spins ($1,\ 1/2$) on 2D lattice structures (hexagonal, square). The transition for all NPs corresponds to a second-order phase transition in the absence of magnetic field ($h \approx 0$). The spin disorder can be caused by lower coordination of the surface atoms in core-surface NPs broken exchange interactions that produce spin-glass (SG) like state of spatially disordered spin in the surface captions with inhomogeneous surface effects (Kodama, 1999; Kaneyoshi, 2005). Our theoretical observations are scrutinized below briefly.

i. All critical temperature ($\sqrt{T_C}$) values of both types of Ising NPs on 2D lattice structures follow a linear increase with the particle size. With increase in the NP size it approaches to the Crue temperature of the bulk materials. These results agree with the mean-field magnetic structure of Heisenberg NPs (Usov & Gudoshnikov, 2005).
ii. From the hysteresis loops for the homegeneous $S = 1/2$ and $S = 1$ Ising NPs which have different sizes and corresponding coercive field (h_C) vs. R^{-2} variations, it is clearly seen that the coercivity strongly depends on the particle size. Due to the superparamegnetic regime the hysteresis curves of small diameters are almost independent of each other while the curves of big diameters sharply change. This shows that the NP approaches to bulk materials.
iii. The hysteresis loops at different temperatures show a monotonic change in the coercive field of composite Ising NPs on 2D lattice structures. This property probably is an important aspect in the future high-density magnetic data storage.

6. Acknowledgements

One of us (Orhan Yalçın) would like to express his gratitude to "The Scientific and Technological Research Council of Turkey" (TÜBİTAK) for financial support (Grant No. 107T635) during the this work.

7. References

Achiam, Y. (1985). Critical Relaxation of the One-Dimensional Blume-Emery-Griffiths Model. *Physical Review B,* Vol.31, pp.260-265, ISSN:1095-3795.

Aktaş, B.; Tagirov, L. & Mikailov, F. (October, 2006). *Magnetic Nanostructures,* Springer Series in materials science, Vol. 94, ISBN 978-3-540-49334-1.

Aktaş, B.; Tagirov, L. & Mikailov, F. (2004). *Nanostructures Magnetic Materials and Their Applications.,* Kluwer Academic Publisher. Nato Science Series. Mathematics, Physics and Chemistry. Vol. 143. ISBN 1-4020-2004-X.

Albayrak, E. (2007). Mixed Spin-2 and Spin-5/2 Blume–Emery–Griffiths Model. *Physica A*, Vol. 375, pp. 174-184, ISSN:0378-4371.

Albayrak, E. (2007). The Critical and Compensation Temperatures for the Mixed Spin-3/2 and Spin-2 Ising Model. *Physica B,* Vol. 391, pp. 47-53, ISSN: 0921-4526.

Albayrak, E. & Yigit, A. (2005). The Critical Behavior of the Mixed Spin-1 and Spin-2 Ising Ferromagnetic System on the Bethe lattice. *Physica A*, Vol. 349, pp. 471-486, ISSN:0378-4371.

Albayrak, E. & Yigit, A. (2006). Mixed Spin-3⁄2 and Spin-5⁄2 Ising System on the Bethe Lattice. *Physics Letters A,* Vol. 353, pp. 121–129, ISSN: 0375-9601.

Bakkali, A.; Kerouad, M. & Saber, M. (1996). The Spin-3/2 Blume-Emery-Griffiths Model. *Physica A,*Vol. 229, No.3-4, pp.563-573, ISSN:0378-4371.

Babin, V.; Garstecki, P. & Holyst, R. (2003). Multiple Photonic Band Gaps in the Structures Composed of Core-Shell Particles. *Journal of Applied Physics,* Vol. 94, pp. 4244, ISSN: 1089-7550.

Benayad, N. & Dakhama, A. (1997). Magnetic Properties of the Mixed-Spin Ising Ferromagnet with a Ferrimagnet Surface. *Physical Review B,* Vol. 55, No.18, pp. 12276-12289, ISSN:1095-3795.

Bakchich, A.; Bekhechi, S. & Benyoussef, A. (1994). Multicritical Behavior of the Antiferromagnetic Spin-3/2 Blume-Capel Model. *Physica A,* Vol. 210, pp. 415-423, ISSN:0378-4371.

Bakuzis, A.F. & Morais, P.C. (2004). Magnetic nanoparticle systems: an Ising model approximation *Journal of Magnetism and Magnetic Materials,* Vol.272-276, pp. e1161-e1163 ISSN: 0304-8853.

Blume, M. (January 1966). Theory of the First-Order Magnetic Phase Change in UO_2, *Physical Review*, Vol. 141, No.2, pp. 517-524, ISSN 1094-1622.

Blume, M.; Emery, V. J. & Griffiths, R. B. (September 1971). Ising Model for the λ Transition and Phase Separation in He^3-He^4 Mixtures, *Physical Review A*, Vol. 4, No.3, pp. 1071-1077, ISSN 1094-1622.

Capel, H. W., (1966). On the Possibility of First-Order Phase transitions in Ising Systems of Triplet Ions with Zero-Field Splitting. Physica Vol. 32, pp. 966-988.

Chen, H.H. & Levy, P.M. (1973). High Temperature Series Expansions for a Spin-1 Model of Ferromagnetism, *Physical Review B*, Vol. 7, pp. 4284–4289, ISSN: 1538-4446.

Çiftçi, N. (July, 2011). *Magnetic properties of a monodomain nanoparticle with dipole-quadropole interaction*, Master of Science Thesis. Thesis Supervisor, R. Erdem. Gaziosmanpaşa University, Turkey.

Deviren, B.; Keskin, M.& Canko, O. (2009). Kinetics of a Mixed Spin-1/2 and Spin-3/2 Ising Ferrimagnetic Model. *Journal of Magnetism and Magnetic Materials*, Vol. 321, pp. 458–466,. ISSN: 0304-8853.

Deviren, B.; Keskin, M. & Canko, O. (2009). Magnetic Properties of an Anti-ferromagnetic and ferrimagnetic Mixed Spin-1/2 and Spin-5/2 Ising Model in the Longitudinal Magnetic Field within the Effective-Field Approximation. *Physica A*, Vol. 388, pp. 1835-1848, ISSN:0378-4371.

Erdem, R. (2009). Frequency Dependence of the Complex Susceptibility for a Spin-1 Ising Model. *Journal of Magnetism and Magnetic Materials*, Vol. 321, pp. 2592–25595,. ISSN: 0304-8853.

Erdem, R. & Keskin, M. (2001). Dynamics of a Spin-1 Ising System in the neighborhood of Equilibrium States. *Physical Review E,* Vol. 64, pp. 0261102-1-9, ISSN 1550-2376.

Erdem, R. (2008). Magnetic Relaxation in a Spin-1 Ising Model near the second-order Phase Transition Point. *Journal of Magnetism and Magnetic Materials*, Vol. 320, pp. 2273–2278,. ISSN: 0304-8853.

Erdem, R. (September, 1995) *A study of the dynamics of a spin-1 Ising model with bilinear and biquadratic interactions.* Science Thesis. Thesis Supervisor, M. Keskin. Gaziosmanpaşa University, Turkey.

Erdinç, A. & Keskin, M. (May 2002). Equilibrium and Nonequilibrium Behavior of the Spin-1 Ising Model in the Quadrupole Phase. *Physica A*, Vol. 307, No. 3-4, pp. 453-468, ISSN:0378-4371.

Fraerman, A. A.; Gusev, S.A.; Nefedov, I.M.; Nozdrin, Y.N.; Karetnikova, I.R.; Mazo L.A.; Sapozhnikov, M.V.; Shereshevsky, I.A. & Suhodoev, L.V. (2001). *Journal of Physics Condensed Matter*, Vol. 13, pp. 683-689. ISSN 1361-648X.

Goveas, N. & Mukhopadhyay, G. (1997). Study of Blume-Emery-Griffiths Model by a Modified Bethe-Peierls Method. *Physica Scripta, Vol.* 56, pp.661-666, ISSN: 0031-8949.

Heisenberg, W. (1928). Theory of ferromagnetism *Zeitschrift für Physik*. Vol. 49, pp. 619-636.

Hoston, W. & Berker, A. N. (1991). Multicritical Phase Diagrams of the Blume-Emery-Griffiths Model with Republisive Biquadratic Coupling. *Physical Review Letters,* Vol.67, pp.1027-1030. ISSN:0031-9007.

Ising, E. (1925). Beitrag zur Theorie des Ferromagnetismus. *Zeitschrift für Physik,* Vol. 31, pp. 253-258.

Kaneyoshi, T.; Nakamura, Y. & Shin, S. (1998). A Diluted Mixed Spin-2 and Spin-5/2 Ferrimagnetic Ising System; A Study of a Molecular-Based Magnet. *Journal of Physics: Condensed Matter,* Vol.10, pp. 7025-7035. ISSN: 1361-648X.

Kartopu G. & Yalçın O., (February, 2010). Electrodeposited Nanowires and their Applications, In: *Electrodeposited Nanowires and Their Applications,* Nicolate Lupu, pp. 113-140. ISBN 978-953-7619-88-6.

Keskin, M.; Ekiz, C. &Yalcin, O. (1999). Stable, Metastable and Unstable Solutions of the Blume-Emery-Griffiths Model. *Physica A*, Vol. 267, pp. 392-405, ISSN:0378-4371.

Keskin, M. (1986). A Model for Quenching Via Hidden Variables Non-Equilibrium Behaviour of a system with Two Range Order Parameters II. Influence of a Magnetic Field. *Physica A,* Vol. 135, pp. 226-236, ISSN:0378-4371.

Keskin, M. & Erdem, R. (1997). Dynamic Behavior of a Spin-1 Ising Model. I. Relaxation of Order Parameters and the 'Flatness' Property of Metastable States. *Journal of Statistical Physics,* Vol. 89, pp. 1035-1046, ISSN: 1572-9613.

Keskin, M. & Erdinç, A. (1995). The Spin-1 Ising Model on the Body-Centered Cubic Lattice Using the Pair Approximation. *Turkish Journal of Physics*, Vol.19, pp. 88-100, ISSN 1010-7630.

Keskin, M. & Meijer, P. H. E. (December 1986). Dynamics of a Spin-1 Model with the Pair Correlation. *Journal of Chemical Physics*, Vol. 85, pp.7324-7333. ISSN: 1520-5207.

Kikuchi, R. (1951). A Theory of Cooperative Phenomena. *Physical Review,* Vol. 81, pp. 988-1002, ISSN: 1536-6065.

Kaneyoshi, T. (2005). Phase Diagrams of a Nanoparticle Described by the Transverse Ising Model. P*hysica Status Solidi (b)* Vol.242, pp. 2938-2948, ISSN: 1521-3951.

Kikuchi, R. (1974). Superposition Approximation and Natural İteration Calculation in Cluster-Variation Method. *Journal of Chemical Physics,* Vol. 60, pp. 1071, ISSN:1089-7690.

Kodama, R.H. (1999)., Magnetic Nanoparticles. *Journal of Magnetism and Magnetic Materials,* Vol.200, pp. 359–372, ISSN:0304-8853.

Kodama, R.H. & Berkowitz, A.E. (March 1999). Atomic-Scale Magnetic Modeling of Oxide Nanoparticles. *Physical Review B, Vol.*59, No. 9, pp. 6321-6336, ISSN:0163-1829.

Kodama, R.H.; Berkowitz, A.E.; McNiff Jr. E.J. & Foner S. (July 1996). Surface Spin Disorder in $NiFe_2O_4$ Nanoparticles. *Physical Review Letters,* Vol.77, No.2, pp.394-397, ISSN:1079-7114.

Leite, V. S. & Figueiredo, W. (2004). Monte Carlo Simulations of Antiferromagnetic Small Particles. *BrazilianJournal of Physics,* Vol. 34, No. 2a, pp.452-454, ISSN 0103-9733.

Meijer, P. H. E.; Keskin, M. & Bodegom, E. (October 1986). A Simple Model for the Dynamics Towards Metastable States. *Journal of Statistical Physics,* Vol. 45, No1-2. pp. 215-232. ISSN: 1572-9613.

Özüm, S. (July, 2010). *A study with pair approximation of spin- Ising model of noninteracting nanoparticles with quadratic and crystal field interactions*, Master of Science Thesis. Thesis Supervisor, Yalçın, O. Bozok University, Turkey.

Peierls, R. (1936). On Isings Model of Ferromagnetism. *Proceedings of the Cambridge Philosophical Society,*.Vol. 32, pp. 477-481, ISSN: 1469-8064.

Pankhurst, Q. A.; Connolly, J.; Jones, S.K. & Dobson, J. (2003). Applications of magnetic nanoparticles in biomedicine. *Journal of Physics D Applied Physics,* Vol. 36,pp. R167, ISSN:1361-6463.

Rego, L. G. C. & Figueiredo, W. (September 2001). Magnetic Properties of Nanoparticles in the Bethe-Peierls Aproximation. *Physical Review B*, Vol. 64, pp. 144424-1-7, ISSN: 1538-4446.

Stoner, E. C. & Wohlfarth, E. P. (1948). A Mechanism of Magnetic Hysteresis in Heterogeneous Alloys. *Philosophical Transactions of the Royal Society of London Series A*, Vol. 240,pp. 599-642, ISSN:0261-0523.

Szlaferek, A. (May 2004). Model Exchange-Spring Nanocomposite Magnetic Grains. *Physica Status Solidi B,* Vol. 241, pp. 1312-1315, ISSN: 1521-3951.

Temizer, U.; Kantar, E.; Keskin, M. & Canko, O. (2008). Multicritical Dynamical Phase Diagrams of the Kinetic Blume–Emery–Griffiths Model with Repulsive Biquadratic Coupling in an Oscillating Field. *Journal of Magnetism and Magnetic Materials*, Vol. 320, pp. 1787–1801, ISSN: 0304-8853.

Usov, N. A. & Gudoshnikov, S. A. (2005). Magnetic Structure of a Nanoparticle in Mean-Field Approximation. *Journal of Magnetism and Magnetic Materials,* Vol.290, pp. 727-730, ISSN: 0304-8853.

Vargas, P.; Altbir, D.; Knobel, M. & Laroze, D. (May 2002). Thermodynamics of Two-Dimensional Magnetic Nanoparticles. *Europhysics Letters,* Vol.58, No. 4, pp. 603-609, ISSN:1286-4854.

Wernsdorfer, W.; Hasselbach, K.; Mailly, D.; Barbara, B.; Benoit, A.; Thomas, L. & Suran, G. (1995). DC-SQUID Magnetization Measurements of Single Magnetic Particles. *Journal of Magnetism and Magnetic Materials,* Vol.145, pp. 33, ISSN:0304-8853

Wernsdorfer, W.; Mailly, D. & Benoit, A. (May 2000). Single Nanoparticle Measurement Techniques. *Journal of Applied Physics,* Vol. 87, No. 9, pp. 5094-5096, ISSN: 1089-7550.

Yalçın, O.; Erdem, R. & Övünç, S. (2008). Spin-1 Model of Noninteracting Nanoparticles. *Acta Physica Polonica A*, Vol. 114, No.4, pp. 835-844, ISSN: 0587-4246.

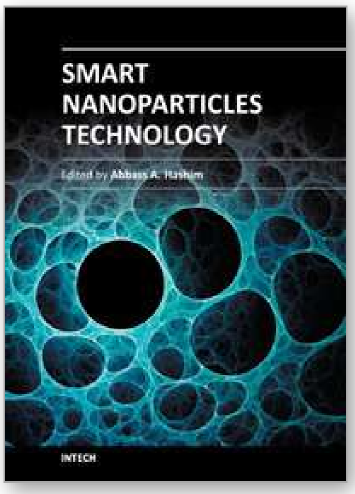

Smart Nanoparticles Technology
Edited by Dr. Abbass Hashim

ISBN 978-953-51-0500-8
Hard cover, 576 pages
Publisher InTech
Published online 18, April, 2012
Published in print edition April, 2012

In the last few years, Nanoparticles and their applications dramatically diverted science in the direction of brand new philosophy. The properties of many conventional materials changed when formed from nanoparticles. Nanoparticles have a greater surface area per weight than larger particles which causes them to be more reactive and effective than other molecules. In this book, we (InTech publisher, editor and authors) have invested a lot of effort to include 25 most advanced technology chapters. The book is organised into three well-heeled parts. We would like to invite all Nanotechnology scientists to read and share the knowledge and contents of this book.

InTech Europe
University Campus STeP Ri
Slavka Krautzeka 83/A
51000 Rijeka, Croatia
Phone: +385 (51) 770 447
Fax: +385 (51) 686 166
www.intechopen.com

InTech China
Unit 405, Office Block, Hotel Equatorial Shanghai
No.65, Yan An Road (West), Shanghai, 200040, China
中国上海市延安西路65号上海国际贵都大饭店办公楼405单元
Phone: +86-21-62489820
Fax: +86-21-62489821